5944 *Macromolecules* **1997,** *30,* 5944−5952

Self-Consistent-Field Modeling of Polyelectrolyte Adsorption on Charge-Regulating Surfaces

Victor Shubin[†] **and Per Linse***

Physical Chemistry 1, Center for Chemistry and Chemical Engineering, Lund University, P.O. Box 124, S-221 00 Lund, Sweden

Received March 11, 1997; Revised Manuscript Received June 16, 1997[⊗]

ABSTRACT: An extension of the self-consistent-field (SCF) lattice theory of polyelectrolyte adsorption, which takes into account electrochemical equilibria at an interface (charge regulation), is presented. The extension consists of replacement of the usual boundary condition of constant surface charge or potential by a charge-potential relation derived from the surface electrochemical equilibria. Most parameters of the model were based on characteristics of real systems, with minimal number of fitting parameters. Theoretical calculations of surface charge density, adsorbed amount, and degree of surface charge compensation by polyelectrolytes as a function of pH and electrolyte concentration were carried out. The results were compared with experimental data. The extended SCF model describes well (at a quantitative level) the surface charge density of the substrate both in the absence and in the presence of adsorbed polyelectrolyte. The theory is also successful in prediction of the main features of the surface charge overcompensation upon polyelectrolyte adsorption under different electrolyte conditions (pH, c_s). By contrast the adsorbed amount is poorly predicted. We believe that the discrepancies between the experiment and the theory are mostly due to nonequilibrium aspects of the polyelectrolyte adsorption, which are not described by the present equilibrium theory.

I. Introduction

Polyelectrolyte adsorption at charged interfaces has numerous industrial applications. Polyelectrolytes are used for surface modification of disperse systems, mostly in order to affect their stability. A detailed understanding of the mechanism of the adsorption process and of the influence of different factors on the properties of adsorbed layers is clearly important for optimal use of polyelectrolytes.

The multiplicity of applications of polyelectrolyte adsorption stimulated much attention to the topic over the last 2 decades. A recent review by Fleer et al.[1] covers experimental techniques used to investigate kinetics of the adsorption, characteristics of the adsorbed layers, and experimental findings accumulated in literature over the past years. On the theoretical side, the adsorption of polyelectrolytes at large surfaces and on colloidal particles has been a subject of great interest as well. Beside (semi)analytic theories of polyelectrolyte adsorption,[2−5] theoretical approaches as numerical solutions of mean-field models[4,6−13] and Monte Carlo simulations[3,14,15] have been applied during recent years.

The main factors governing adsorption of polyelectrolytes on charged surfaces from solution are the molecular weight of the polymer, its linear charge density, the charge distribution along the polyelectrolyte chain, substrate charge, the ionic strength of the solution, and the nonelectrostatic affinity of counterions and polyelectrolyte to the surface. All the above factors are well accounted for in recent versions of self-consistent-field (SCF) theory of polyelectrolyte adsorption[7,11,16] based on the mean-field lattice model of polymer adsorption developed by Scheutjens and Fleer.[17,18]

Extensive numerical investigations of polyelectrolyte adsorption onto oppositely charged surfaces within the SCF approach[10,12] show that theoretical predictions are in qualitative agreement with a number of experimental trends. Mean-field lattice theory appears to be successful in qualitative modeling of the adsorption in several different polyelectrolyte-containing systems. Among them are weak polyacid on constant-charge latexes,[19] highly charged polyelectrolyte on neutral surface,[20] cationic amylopectin on microcrystalline cellulose,[21] and cationic polyacrylamide on silica.[13] However, in all cases the substrates have been modeled either as constant-charge (σ_0 = const) or as constant-potential (ψ_0 = const) surfaces. This has been so even in cases[13,21] when neither condition strictly holds. In practice, surfaces that regulate their surface charge are ubiquitous, e.g., metal oxides and aluminosilicates, cellulose and its derivatives, biocolloids, and some synthetic latexes. Such surfaces bear dissociable functional groups whose degree of dissociation depends on the conditions in the solution. Then, in general, neither surface charge nor surface potential remains constant with changes in solution physicochemical properties. In this case either the surface charge density or the surface potential used in theoretical calculations must be determined independently or the electrochemical equilibrium at the interface (charge regulation) should be modeled within the same theoretical approach as the polyelectrolyte adsorption.

Charge regulation on metal oxides and similar surfaces, where H^+ and OH^- are the potential-determining ions, is widely modeled within the framework of a theoretical approach based on an earlier works by Ninham and Parsegian,[22] Levine and Smith,[23] further developed by Healy and White,[24] Davis et al.,[25] Davis and Leckie,[26] and finally reviewed and elaborated by James and Parks.[27] This approach, which is usually referred to as a triple-layer or site-binding model (SBM), attributes the surface charge formation to two types of reactions: (i) dissociation of discrete surface functional groups and (ii) complexation (specific adsorption) of electrolyte ions on particular surface sites. Mass-action equations for the surface equilibria, supplemented by charge electroneutrality and mass balance conditions, as well as by charge-potential relations that follow from

---

* The author to whom all correspondence should be addressed.

[†] Permanent address: Department of Colloid Chemistry, Chemical Faculty, St. Petersburg University, 198904 St. Petersburg, Russia.

[⊗] Abstract published in *Advance ACS Abstracts,* August 15, 1997.

S0024-9297(97)00334-3 CCC: $14.00

the electrical double layer (EDL) model adopted, provide a set of equations which can be solved numerically to produce all EDL parameters, including σ_0 and ψ_0. The original papers quoted above provide more details.

The major problem in applying the SBM to real systems is the proper choice of model parameters (intrinsic constants of surface reactions, surface sites density, EDL structural characteristics). As has been shown by Koopal et al.,[28] an appropriate way of determining the parameters can be found provided a sufficient amount of experimental information on the electrochemical behavior of a system is available. This granted, the site-binding model can be used successfully to model charge regulation at solid/liquid interfaces when the solution contains only simple ions. It is known, however, that adsorption of polyelectrolytes substantially affects the substrate charge,[29−33] and this requires further theoretical developments.

Recently, an extension of the SBM to systems containing low molecular-weight polyelectrolyte was proposed by Dupont and Foissy.[34] Although the approach has an advantage of simplicity and proved to be adequate in prediction of the adsorption and charge formation trends, the model presented by the authors is restricted to short-chain polyelectrolytes which adsorb in a flat conformation. In the case of long-chain polyelectrolytes, conformational effects play an important role in the adsorption process and have to be considered.

We shall show in the present paper that extension of the self-consistent-field lattice theory by incorporation of surface chemical equilibria can be performed in a straightforward manner and we shall present results of model calculations of polyelectrolyte adsorption on charge-regulating surfaces. As far as possible, the values of the model parameters are taken from known properties of the system modeled or obtained from fits to experimental data for simpler systems. The results of the modeling will then be compared with experimental data recently obtained by Shubin et al.[32,33] Self-evidently, in order to test any model of polymer adsorption, one should use experimental results obtained with well-defined model systems. This requires the use of (i) polymers of high purity with known concentration of functional groups and narrow distribution of molecular weight and (ii) substrates with simple geometry and known surface composition (i.e., known density and chemical nature of surface functional groups). The experimental data we explore in the present paper do meet the above requirements.

II. Experimental Background

The model calculations are based on experimental measurements on (i) monodisperse nonporous silica and low linear charge density cationic polyacrylamide[32] and (ii) monodisperse carboxyl-functionalized polystyrene latex and medium linear charge density cationic polyacrylamide.[33] For both systems measurements of (i) substrate charge density in the absence and in the presence of adsorbed polyelectrolyte obtained by potentiometric titration and (ii) adsorbed amount of polyelectrolyte obtained by polyelectrolyte titration have been performed. These measurements were made over a wide range of pH and background electrolyte (KCl) concentrations c_s. The polymers used in these studies have the same chemical nature, being copolymers of acrylamide (AM) and ((3-methacrylamido)propyl)trimethylammonium chloride (MAPTAC). They differ only in the fraction of charged segments (τ). The polyelectrolytes carry a constant positive charge due to quaternary ammonium groups on the MAPTAC units. The surface charge of the substrates, originating from dissociation of silanol (for silica) and carboxylic (for latex) groups, is negative and pH- and c_s-dependent. The main characteristics of the two systems are listed in Table 1. This includes estimates of dissociation (K_a) and cation-binding (K_K) constants obtained from σ_0 *vs* (c_s, pH) data for these systems by Shubin et al.[32,33] using a graphical extrapolation technique developed within the site-binding model.[28,35]

Table 1. Main Characteristics of the Experimental Systems

	polyelectrolyte	
	system 1	system 2
τ	0.034[a]	0.33[a]
M_w	10^6 [b]	10^6 [b]

	substrate	
	silica	latex
ϕ (nm)	300[c]	340[c]
σ_0^{max} (C/m^2)	0.8[d]	0.149[e]
pK_a	8.1[f]	4.8[g]
pK_K	−0.6[f]	−0.1[f]

[a] Determined by polyelectrolyte titration. [b] Specified by the manufacturer. [c] Particle diameter measured by TEM. [d] Estimated elsewhere.[44] [e] Measured by potentiometric titration. [f] Estimated from $\sigma_0 = f(c_s, \text{pH})$ data via double-extrapolation technique. [g] Assumed to be equal to pK_a of a long-chain carboxylic acid.

III. Theoretical Approach

Extension of the SCF Theory to Adsorption on Charge-Regulating Surfaces. In the self-consistent mean-field lattice theory the half-space next to a surface is divided into parallel layers of thickness *d* (lattice spacing) and each layer is further divided into lattice cells of equal size. One lattice cell contains either solvent (or a cluster of solvent molecules), a solvated ion, or a polymer segment. The polyelectrolyte is considered to be a completely flexible chain, consisting of *r* polymer segments of which a fraction τ is charged. One segment is not necessarily equal to a monomer, but it is a structural unit of an appropriate size. Thus, in general a model system contains a number of different species: various kinds of polymer segments, ions, and solvent. The treatment of the polyelectrolyte as a completely flexible chain is obviously a major simplification. Recent Monte Carlo studies address the issue of chain entropy on the overal extension of the polyelectrolyte.[36]

In the mean-field approach all species are assumed to interact with a potential of mean force with respect to a reference state which is taken to be the bulk solution. This implies that all lattice sites in a given layer parallel to the planar surface are equivalent. Three contributions to the potential of mean force are considered in the theory. The first contribution is due to short-range interactions between species in adjacent lattice sites. These are taken into account through Flory−Huggins χ parameters. The same description is used for the interaction with the surface. For example, for neutral polymer segments the adsorption parameter χ_n is given by $\chi_n = -\lambda_{1,0}(\chi_{n,s} - \chi_{w,s})$ where $\chi_{n,s}$ and $\chi_{w,s}$ are Flory−Huggins parameters for neutral segment−surface and solvent−surface interaction, respectively, and $\lambda_{1,0}$ is the fraction of all neighbors of a site in layer 1 which resides in the surface layer ($\lambda_{1,0} = {}^1/_3$ for the face-centered cubic lattice used in the present work). The second contribution arises from long-range electrostatic (charge−charge) interactions. The electrostatic potential of mean force is related to the charge density through the discrete version of the Poisson equation. A uniform dielectric constant $\epsilon_r = 80$ is used. The third potential component is due to hard core interactions. It is species independent and ensures full occupancy of each lattice layer.

The configuration of a polyelectrolyte molecule is modeled as a weighted random walk on the lattice, where the Boltzmann weight of the potential of the mean force that contains the contributions described above occurs as a weighting factor. For details, and for the numerical procedure for solving the resulting set of implicit equations self-consistently, we refer to the original sources (e.g., ref 16). Up to this point the model is the same as that described in our recent publications.[10,13]

In order to take into account the electrochemical equilibrium at the solid−solution interface and to go beyond the simplifying condition of constant surface charge or constant surface potential, we now introduce a concept of surface chemical reactions in a way similar to that adopted in the SBM. We consider a system consisting of a functionalized surface (e.g., bearing SOH monofunctional dissociable groups) immersed in electrolyte solution (say, KCl) containing polyelectrolyte with charged segments P$^+$. We assume that the three following reactions take place controlling the surface charge density:

$$\mathrm{SOH} \overset{K_a}{\longleftrightarrow} \mathrm{SO}^- + \mathrm{H_0}^+ \tag{1}$$

$$\mathrm{SO}^- + \mathrm{K_1}^+ \overset{K_K}{\longleftrightarrow} \mathrm{SO^-K^+} \tag{2}$$

$$\mathrm{SO}^- + \mathrm{P_1}^+ \overset{K_P}{\longleftrightarrow} \mathrm{SO^-P^+} \tag{3}$$

As in the SBM, we assume that the adsorption of protons occurs in a “zero” plane where the functional groups are located and where the electrostatic potential is Ψ_0, while bound counterions and charged polyelectrolyte segments are located in the first lattice layer where the electrostatic potential is Ψ_1. The subscripts on the ionic species symbols reflect this arrangement. The assumption is based on simple arguments: a proton, if not released into solution, forms a part of the functional group, whereas a counterion or a charged polyelectrolyte segment has a certain size. Upon adsorption it partially retains its hydration shell and may even share hydration water with the surface, as was suggested in ref 37.

Each of the above reactions is characterised by a corresponding intrinsic equilibrium constant

$$K_a = \frac{[\mathrm{SO}^-][\mathrm{H}^+]_0}{[\mathrm{SOH}]} \tag{4}$$

$$K_K = \frac{[\mathrm{SO^-K^+}]}{[\mathrm{SO}^-][\mathrm{K}^+]_1} \tag{5}$$

$$K_P = \frac{[\mathrm{SO^-P^+}]}{[\mathrm{SO}^-][\mathrm{P}^+]_1} \tag{6}$$

with [···] denoting the concentration. The surface charge density is given by

$$\sigma_0 = -e([\mathrm{SO}^-] + [\mathrm{SO^-K^+}] + [\mathrm{SO^-P^+}]) \tag{7}$$

and the mass balance condition is given by

$$N_s = [\mathrm{SOH}] + [\mathrm{SO}^-] + [\mathrm{SO^-K^+}] + [\mathrm{SO^-P^+}] \tag{8}$$

where N_s is the surface site density. Then if we relate the proton concentrations in the zero and the first layers via a Boltzman-type equation

$$[\mathrm{H}^+]_0 = [\mathrm{H}^+]_1 \exp(\bar{\Psi}_1 - \bar{\Psi}_0) \tag{9}$$

where $\bar{\Psi} = e\Psi/kT$, from eqs 4−9 we obtain a charge−potential relation:

$$\sigma_0 = eN_s\left[1 + \frac{[\mathrm{H}^+]_1 \exp(\bar{\Psi}_1 - \bar{\Psi}_0)}{K_a(1 + K_P[\mathrm{P}^+]_1 + K_K[\mathrm{K}^+]_1)}\right]^{-1} \tag{10}$$

Our extension of the lattice model consists in replacement of the usual boundary condition (σ_0 = constant or Ψ_0 = constant) with the implicit relation given by eq 10. This is solved by assigning an initial value to σ_0, applying the standard SCF numerical scheme, and obtaining through a conventional Newton−Raphson procedure an improved σ_0 which eventually satisfies eq 10.

Our model system contains six different species in the solution: neutral polymer segment, charged polymer segment, cation, anion, proton, and solvent. A generalization of the charge-regulating model to an arbitrary surface (e.g., amphoteric) and arbitrary number of adsorbing species is straightforward.

IV. Model Parameters

Being multiparametric, the SCF model is rather flexible in a sense that theoretical calculations can predict a large variety of a system behavior depending on the choice of parameters. This means that the modeling can be misleading unless (i) the model reproduces well the main features of a real system (in terms of geometry, composition, and properties of components) and (ii) the number of free fitting parameters is reduced to a minimum. These conditions can be fulfilled if (i) a well-defined (model) system is dealt with and (ii) the available experimental information allows one to make a well-justified choice of the dominating model parameters.

Lattice. A planar lattice was chosen since the radii of the particles (150−170 nm) are much larger than the thicknesses of the adsorbed layers. The choice of the lattice spacing was based mainly on the mean size of the structural units of the polyelectrolytes. The chemical structures of the monomers involved are presented in Figure 1a. The polyelectrolyte can be subdivided into roughly equal sized segments with mean partial molar volume of about 53 cm^3/mol. This was calculated using an assumed additivity for the structural components.[38] This would correspond to a cubic lattice size d = 0.45 nm, which also is realistic with respect to the other components. The maximal surface charge densities in reduced units were calculated with this choice of d and the maximal surface charge densities given in Table 1.

Polyelectrolytes. The polyelectrolytes involved in the experimental systems can be represented as $(\mathrm{AM_{28}MAPTAC})_{N_{b1}}$ and $(\mathrm{AM_2MAPTAC})_{N_{b2}}$, where N_{b1} and N_{b2} are the number of block repetitions per molecule. For

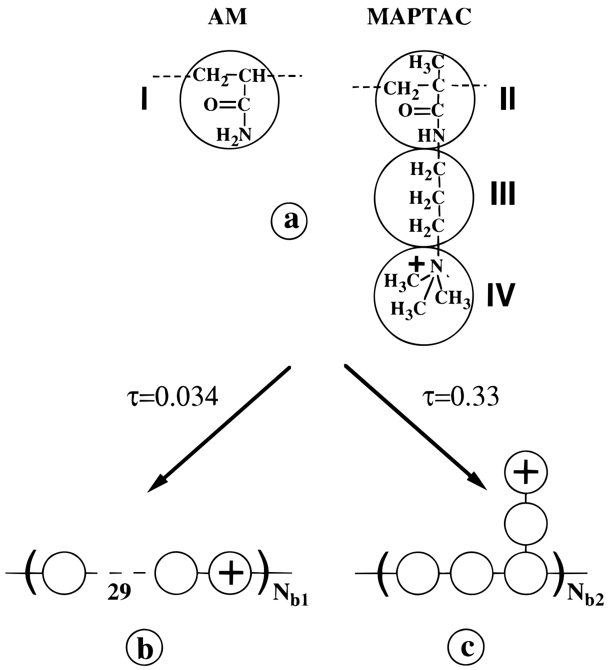

Figure 1. (a) Chemical structure of AM and MAPTAC monomers and the definition of the averaged structural unit: I, $V_0 = 51.2$ cm^3/mol and $M_w = 71$ g/mol; II, $V_0 = 66.0$ cm^3/mol and $M_w = 85$ g/mol; III, $V_0 = 47.4$ cm^3/mol and $M_w = 42$ g/mol; IV, $V_0 = 62.6$ cm^3/mol and $M_w = 59$ g/mol. Averaging over the two types of macromolecules gives $\bar{V}_0 = 53$ cm^3/mol and $\bar{M}_w^s = 80$ g/mol. (b) The model structure of the polyelectrolyte with $\tau = 0.034$. (c) The model structure of the polyelectrolyte with $\tau = 0.33$.

a polymer with $M_w = 10^6$, the corresponding values of N_{bi} would be around 450 and 2700, respectively.

For the low-charge polyelectrolyte, preliminary calculations showed that the detailed description of the MAPTAC unit (side chain) was of no importance, while peculiarities of charge distribution along the chain affected the results. For this polyelectrolyte a linear molecular structure (Figure 1b) with a random distribution of charged segments was adopted. By contrast, for the second polyelectrolyte a regular and a random charge distribution gave essentially identical results, whereas the results were sensetive to the molecular architecture. The second polyelectrolyte was therefore modeled as a branched molecule with a regular charge distribution (Figure 1c). For both polyelectrolytes the total number of segments was ca. 10 000 ($N_{b1} = 350$ and $N_{b2} = 2000$). The slightly lower values of N_{b1} and N_{b2}, as compared with the real polyelectrolytes, is of no consequence for the adsorbed amount.

The theoretical excess amount Γ^{ex} (expressed in equivalent layers) is converted into Γ (mg/m^2) by using a mean segment molecular weight = 80 g/mol. The resulting conversion relation is then $\Gamma = 0.658\Gamma^{ex}$. Finally, the bulk volume fraction of polymer was assumed to be $\phi_p = 5 \times 10^{-5}$, which corresponds to 50 ppm in real systems.

Charge Regulation and Surface Interaction Parameters. The dissociation of surface functional groups and binding of cationic species to the surface sites are described by using virtually the same approach as in the SBM. This allows us to use the values of the dissociation constant K_a and the cation-binding constant K_K estimated from experimental $\sigma_0 = f(c_s, \text{pH})$ data within the SBM (Table 1). The constants K_a and K_K listed in Table 1 are expressed in conventional units: molar and inverse molar concentration, respectively. Conversion of molar concentrations (c) into volume fraction units is made through the equation $\phi = 0.0547c$. Then the equilibrium constants in the model units are given by $pK_a^\phi = pK_a + 1.26$ and $pK_K^\phi = pK_K - 1.26$.

Table 2. Parameters used in Model Calculations

	system 1	system 2
temperature, T (K)	298	
relative dielectric constant, ϵ_r	80	
lattice type	face-centered cubic	
lattice spacing, d (nm)	0.45	
polymer volume fraction, ϕ_p	5×10^{-5}	
fraction of charged monomers, τ	0.034	0.33
number of segments per molecule, r	10150	10000
molecule structure	linear	branched
linear charge distribution	random	regular
maximal surface charge density, σ_0^{max}	−1	−0.188
pK_a^ϕ	9.4	6.1
pK_K^ϕ	−1.8	−1.4
pK_P^ϕ	−1.5	−1.3
$RT\chi_{n,s}$ (kJ/mol)	−5	−4
$RT\chi_{polymer,water}$	$0.5RT$	
$RT\chi_{polymer,cation}$	$0.5RT$	
$RT\chi_{polymer,anion}$	$0.5RT$	

The parameters characterizing the polyelectrolyte−surface interaction, i.e., pK_p^ϕ and χ_n, were used as fitting parameters and we have used the $\sigma_0 = f(c_s, \text{pH})$ data in the presence of polyelectrolyte to determine them. However, their values were not allowed to take unrealistic values. It is known that quaternary ammonium ions normally have a somewhat lower affinity to oxide surfaces than alkali ions.[39] This implies that pK_P^ϕ is expected to be less negative than pK_K^ϕ. Since the strength of nonelectrostatic interaction affects the calculated surface charge density strongly at low pH (low charge), the choice of an appropriate $\chi_{n,s}$ value was quite straightforward. All other surface interaction parameters are set to zero.

Bulk Interaction Parameters. As in previous and similar modeling of polyelectrolyte adsorption,[12,13,19,21] we assumed an unfavorable nonelectrostatic interaction of polymer segments with water and salt species ($\chi = 0.5$). All other bulk interaction parameters were set to zero which means the absence of short-range interaction between corresponding components. All parameters used in the model calculations are compiled in Table 2.

V. Results

Surface Charge Density. Figures 2 and 3 present the calculated surface charge density for the case of the substrate immersed in an electrolyte solution without any polyelectrolyte (dashed curves). The corresponding experimental data are also shown (open symbols) and a good quantitative agreement between the experiment and the theoretical data is obtained for both substrates. This implies that the extended SCF model can adequately describe the charge regulation on real substrates and that the choice of the model parameters is appropriate. At this stage we have not yet used any parameters fitted in the present SCF calculations.

Hence, the mean-field lattice theory with intrinsic constants of reactions 1−2, determined within the site-binding approach, describes the charge formation as good as the SBM does. This is hardly surprising since the description of the surface equilibria in these two theories is identical. The treatment of electrostatics, although somewhat different, turns out to be virtually identical also. In both theoretical formulations the mean-field approximation is adopted. The main differences lies in the fact that in the SBM the potential drop

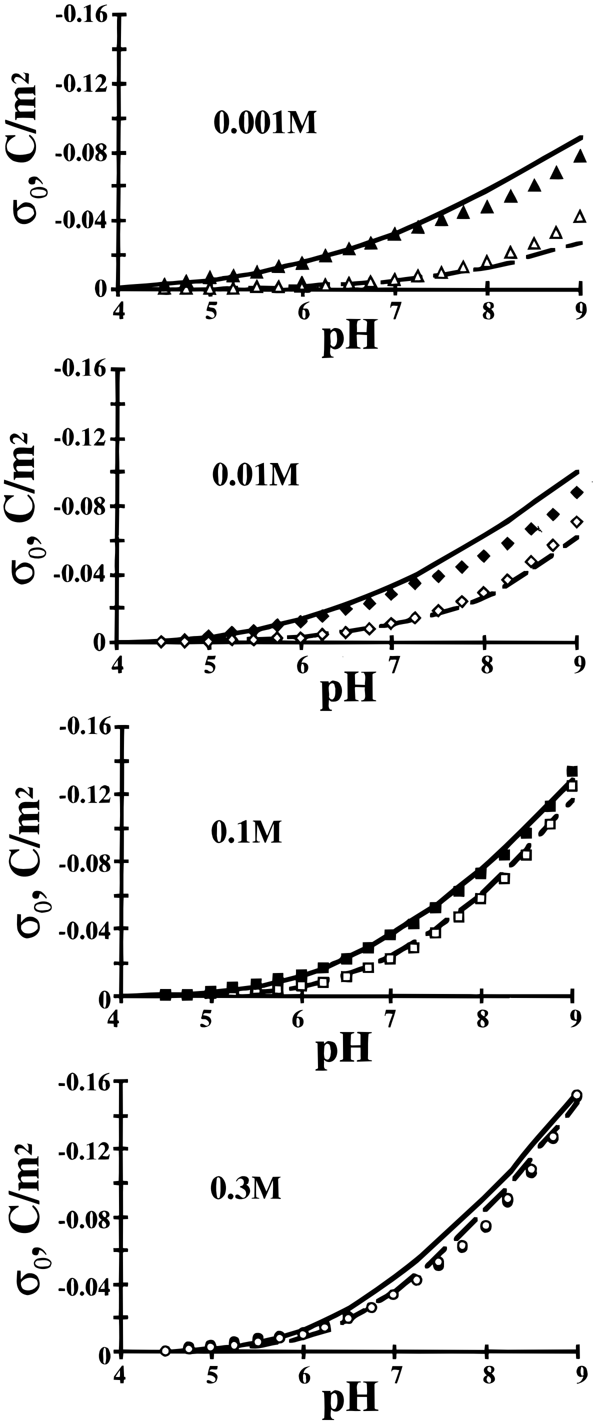

Figure 2. Surface charge density as a function of pH at indicated electrolyte concentrations for system 1 (silica and polyelectrolyte with $\tau = 0.034$) from model calculations in the absence of polyelectrolyte (dashed curves) and in the presence of polyelectrolyte (solid curves) and from experiments in the absence of polyelectrolyte (open symbols) and in the presence of polyelectrolyte (filled symbols).

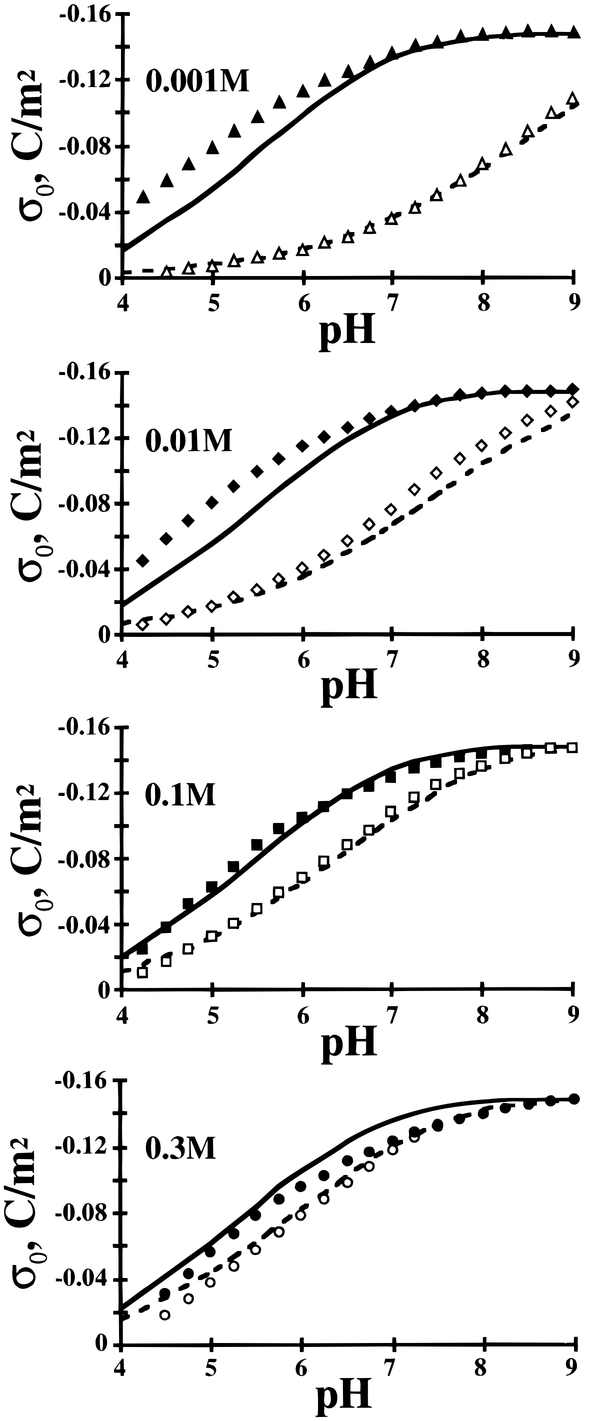

Figure 3. Surface charge density as a function of pH at indicated electrolyte concentrations for system 2 (latex and polyelectrolyte with $\tau = 0.33$) from model calculations in the absence of polyelectrolyte (dashed curves) and in the presence of polyelectrolyte (solid curves) and from experiments in the absence of polyelectrolyte (open symbols) and in the presence of polyelectrolyte (filled symbols).

in the inner part of the Stern layer is given by the formula for a parallel-plate condenser:

$$\Psi_0 - \Psi_1 = \sigma_0/C_1 \tag{11}$$

Here C_1 is the capacitance of this part of the electrical double layer and it is used in the SBM as a fitting parameter. For our systems 1 and 2 it was found to be 1.7 and 2.0 F/m^2, respectively.[32,33] However, in the extended SCF model the charges are located in planes in the center of each lattice layer and the electrostatic potential profile is described by the discrete version of the Poisson−Boltzmann equation. Hence, the potential drop across the first layer is determined by its capacitance $C_1 = \epsilon\epsilon_0/d$. With the model parameters used in our calculations, one obtains $C_1 = 1.6$ F/m^2, which is close to the SBM estimates.

The calculations for systems with adsorbed polyelectrolyte involve two additional important parameters: p$K_P{}^\phi$ and χ_n. These characterize the short-range interaction of charged and uncharged segments of the polymer with the surface and are used as fitting parameters. The best fit of the experimental data (by inspection) was obtained with values of these parameters listed in Table 2. Figures 2 and 3 show the theoretical (solid curves) and experimental (filled symbols) σ_0 *vs* pH dependences at different c_s for both systems. With the chosen parameters, the extended SCF theory reproduces well at a semiquantitative level the surface charging behaviour and the effect of polyelectrolyte on it for both systems.

At low electrolyte concentrations, the magnitude of the surface charge in the presence of adsorbed polyelectrolyte is substantially higher than that of the bare substrate. As the electrolyte concentration increases, the effect of polyelectrolyte adsorption on surface charge diminishes. This feature is in line with the molecular picture of polyelectrolyte adsorption under varied electrolyte conditions, which emerged from previous calculations.[10,13] At low ionic strength the polyelectrolyte molecule tends to adsorb at the surface in a flat conformation, forming numerous contacts with the surface. This yields a high concentration of charged segments in the first layer. Equilibrium 3 is then shifted to the right which shows up as an increase in σ_0 through reaction 1. At higher salt content, the screening of the electrostatic attraction of charged segments to the surface and the competition of the cations for the surface sites result in a more extended interfacial conformation of the macromolecules with fewer points of contact with the surface. This leads to a weaker influence of the polyelectrolyte adsorption on the surface charge density.

The charge increase upon polyelectrolyte adsorption is larger for system 2 as compared to system 1. Apparently, this is due to a cumulative effect of two factors: (i) the higher charge density of the polyelectrolyte implies a flatter interfacial conformation and, concomitantly, a higher concentration of charged segments in the first layer and (ii) higher reactivity (lower pK_a) of the latex surface which facilitates the surface charge adjustment upon polyelectrolyte adsorption as compared to the silica surface.

Adsorbed Amount. Representative results of calculated adsorbed amount as a function of pH and electrolyte concentration are given in Figures 4 and 5 together with corresponding experimental data. Unlike the case of the surface charge density, the agreement between experimental and predicted adsorbed amounts is rather poor.

Not only is the quantitative agreement not good but in many cases the theory fails to predict qualitative trends of the experimental Γ *vs* (c_s, pH) dependences. Especially this is true for system 1. For example, the theory predicts a monotonic increase of adsorbed amount with increase in pH, more strongly pronounced the higher the pH is, while in the experiment an initial steep increase in Γ is followed by a plateau at pH $\geq$ 6 (Figure 4a). At pH < 8 the calculations also do not reproduce the Γ decrease at high c_s (c_s > 0.1 M) observed in experiments (Figure 4b). However, at some other conditions qualitative agreement between the model and the experiment results is much better (Figure 5b,c) or even rather good agreement is observed (Figures 4c and 5a).

Supplementary calculations showed that the overall fit of the experimental data cannot be improved by varying the parameters. This makes it doubtful that unproper choice of model parameters is responsible for the observed discrepancies. Possible explanations will be put forward below.

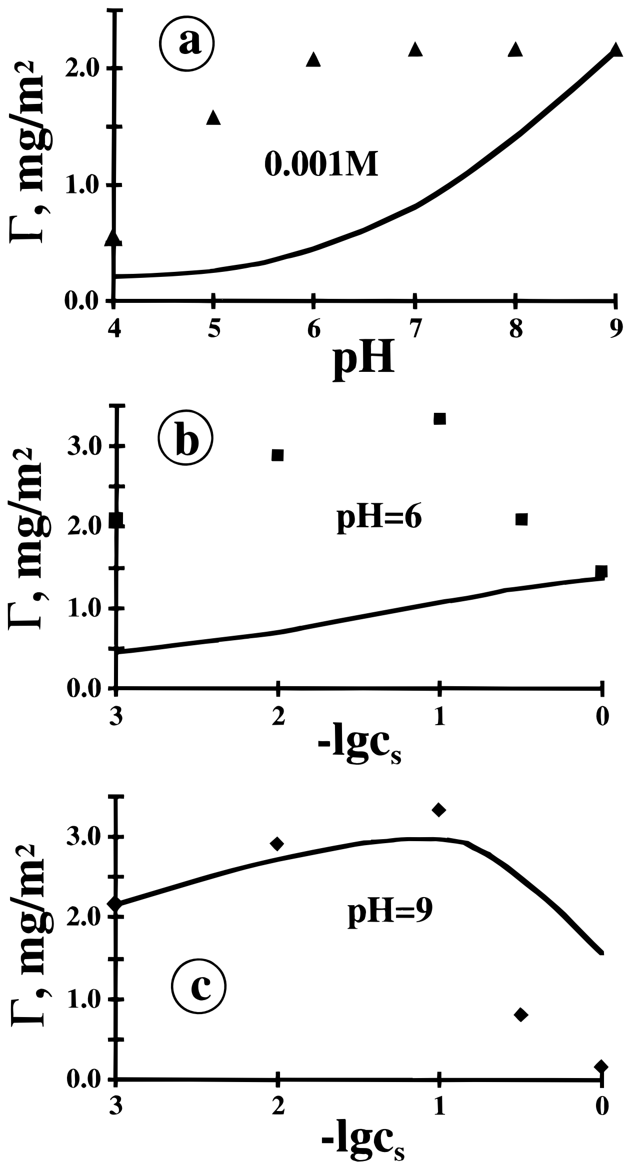

Figure 4. Adsorbed amount of polyelectrolyte as a function of pH at c_s = 0.001 M (a) and as a function of electrolyte concentration at pH = 6 (b) and pH = 9 (c) for system 1 (silica and polyelectrolyte with τ = 0.034) from model calculations (solid curves) and from experiments (symbols).

Charge Balance at the Interface. The ratio of the charge of adsorbed polyelectrolyte and the surface charge, usually referred to as the "charge ratio" *r*, is an important characteristic of the adsorption process. If electrostatics is the only driving force of the adsorption (pure electrosorption), the SCF theory predicts a charge ratio between ca. unity and zero, i.e., the full range of situations between an almost exact charge compensation and a total dispacement of polyelectrolyte by electrolyte ions.[10,12] An undercompensation (*r* < 0) is typical for electrosorption of polyelectrolytes with low τ and at high c_s, i.e., when small ions are more efficient in compensating the surface charge. When attractive short-range interaction of a polymer with substrate is operational, charge reversal can take place (*r* > 1). This has been confirmed experimentally in several studies[32,33,40,41] and has been predicted theoretically.[10,12] To the best of our knowledge, however, to date no com-

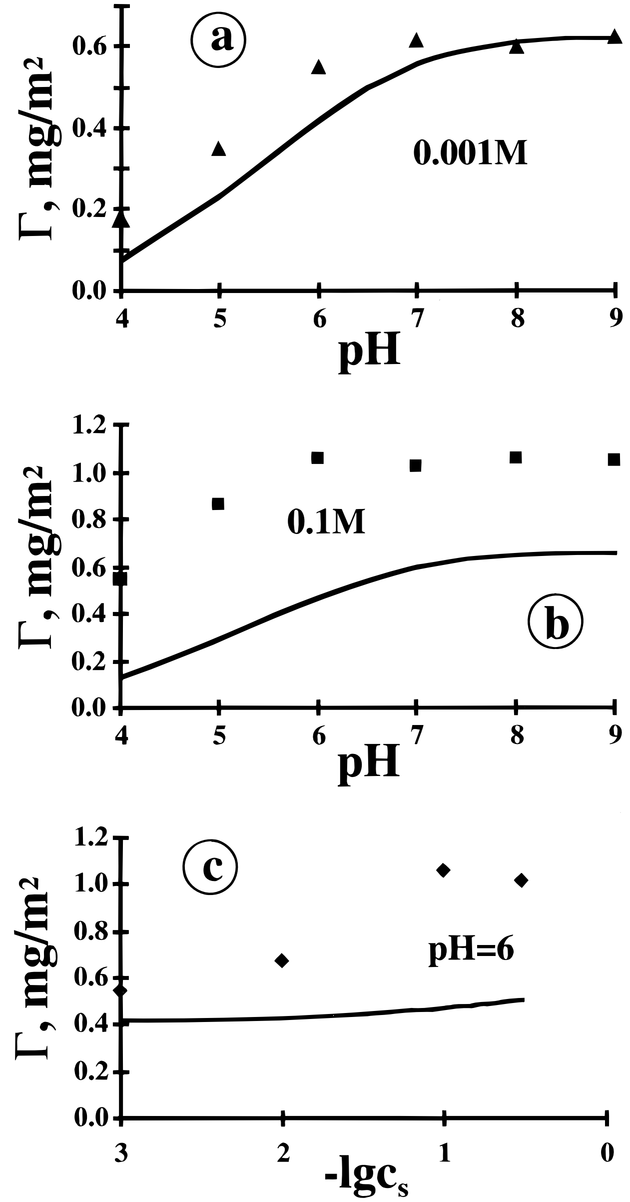

Figure 5. Adsorbed amount of polyelectrolyte as a function of pH at $c_s = 0.001$ M (a) and $c_s = 0.1$ M (b) and as a function of electrolyte concentration at pH = 6 (c) for system 2 (latex and polyelectrolyte with $\tau = 0.33$) from model calculations (solid curves) and from experiments (symbols).

parison of experimental findings with theoretical predictions has been reported in the literature.

Figures 6 and 7 show some representative plots of r as a function of pH and electrolyte concentration. For both systems the r values show very similar qualitative trends: (i) r increases upon decrease in pH at c_s = constant (Figures 6a and 7a) and (ii) at moderate c_s ($c_s \leq 0.1$ M) r increases with increase in electrolyte concentration (Figures 6b and 7b). The overcompensation is normally much more strongly pronounced in system 1 with its more weakly charged polyelectrolyte (cf. the ordinate scales in Figures 6 and 7). For this system another characteristic feature follows from the calculations: undercompensation of the surface charge at high σ_0 and high ionic strength (see Figure 6b, pH = 9). This is due to a partial desorption of the polyelectrolytes at these conditions (cf. the corresponding $\Gamma - c_s$ curve in Figure 4c).

The trends in Figures 6 and 7 can be related to the conformation of the adsorbed molecules. Thus, when the interfacial conformation of a macromolecule is rather flat (high τ, high σ_0, low c_s) the overcompensation is expected to be small since accumulation of the net charge near the surface is highly unfavorable. On the other hand, for expanded adsorbed layers (favored by low τ, low σ_0, and high c_s) an appreciable charge overcompensation is feasible. In this case the surface charge is compensated by the charged segments which are located in the close vicinity to the surface while a large part of the charged segments reside in loops and tails dangling into solution and creates the charge overcompensation. The much stronger charge overcompensation in system 1 is well in line with the tendency of forming expanded layers, typical to low-charge polyelectrolytes.

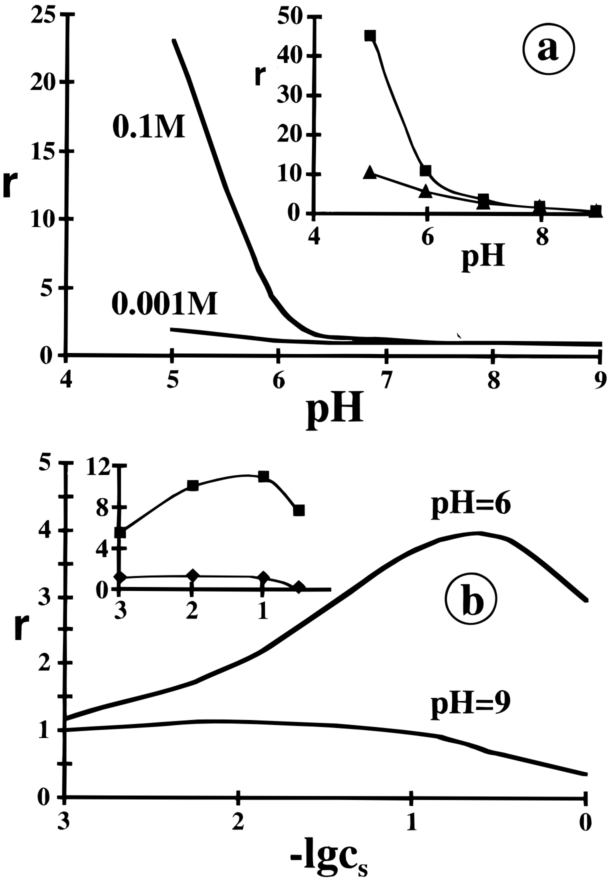

Figure 6. Ratio of adsorbed polyelectrolyte charge to the substrate surface charge as a function of pH (a) and electrolyte concentration (b) for system 1 (silica and polyelectrolyte with $\tau = 0.034$) at indicated conditions from model calculations (main charts) and experiments (inserts).

Comparison of the theoretical predictions with the experimental results given in the inserts of Figures 6 and 7 shows that all the above-described trends have been observed in the experiments. However, despite the striking qualitative agreement between the theory and the experiment, the quantitative difference between the calculated (r^{calc}) and the measured (r^{exp}) values of the charge ratio is rather substantial ($r^{calc} << r^{exp}$). Possible reasons for this discrepancy will be discussed in the following section.

VI. Discussion

As shown in the previous section, the extended SCF theory successfully describes charge formation on substrate surfaces. This means that the theory is adequate with respect to the description of the composition of the

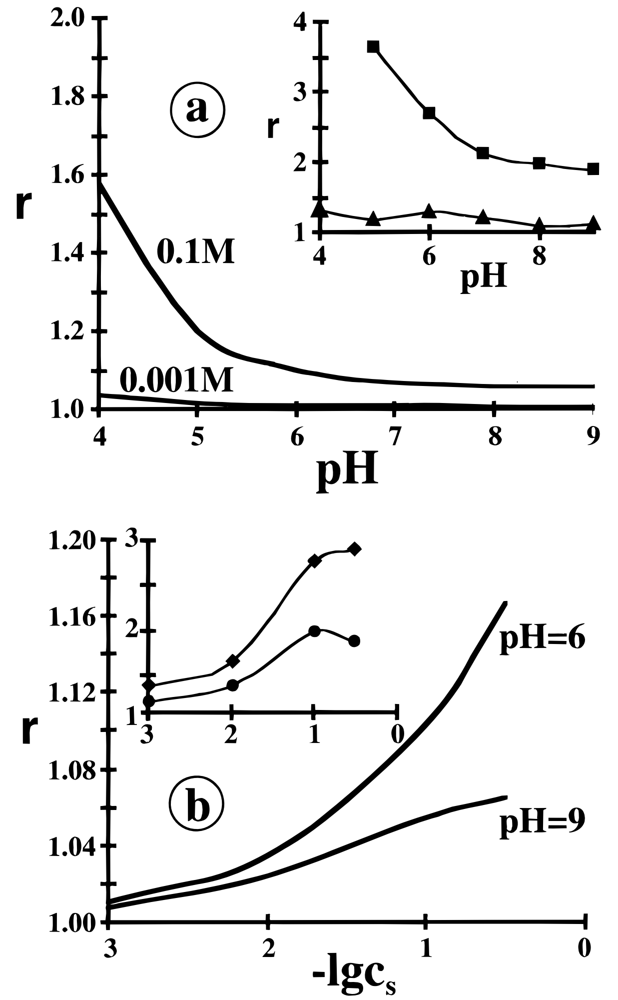

Figure 7. Ratio of adsorbed polyelectrolyte charge to the substrate surface charge as a function of pH (a) and electrolyte concentration (b) for system 2 (latex and polyelectrolyte with $\tau = 0.33$) at indicated conditions from model calculations (main charts) and experiments (inserts).

space immediately adjacent to the surface. At the same time for both systems and for almost all conditions the SCF model substantially underestimates the surface charge overcompensation by adsorbed polyelectrolyte. Apart from possible deficiences in the experimental data (which, however, hardly could produce such a general trend), the reason for such a discrepancy may lie in a mistreatment of the polyelectrolyte conformation at the interface. In other words, our analysis suggests that in reality a larger (as compared to the theory) portion of an adsorbed molecule extends into the liquid phase and a more expanded layer is normally formed.

One of the major simplifications in the treatment of a polyelectrolyte molecule within the present version of the lattice theory is the assumption of a perfect flexibility of the macromolecule. In reality electrostatic repulsion between charged segments imparts a certain rigidity to the chain, characterized by a persistence length. Although this effect, if taken into account, would affect the model predictions, it cannot be solely responsible for the observed discrepances because it is expected to vanish at high ionic strength.

Another possible explanation of the disagreement between the experiment and the model predictions by the equilibrium SCF approach can be connected with manifestations of nonequilibrium features of the adsorption. As was suggested by Vandeven,[42] the adsorbed molecule conformation can be close to that in solution prior to adsorption due to kinetic reasons. The same idea has recently been used by Hoogeveen et al.[43] in the interpretation of their results.

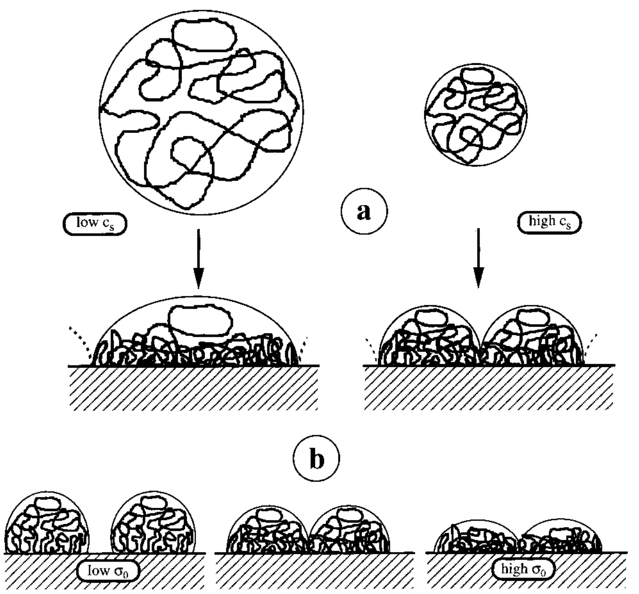

Figure 8. Schematic representation of a mechanism of adsorption, based on the assumption that adsorbing polyelectrolyte molecule partially retains its solution conformation prior to adsorption. The area, occupied by the molecule at the interface (a) is proportional to its expansion in solution. The degree of collapse of the macromolecule bulk conformation upon adsorption depends on both electrolyte concentration (a) and substrate charge (b).

Adopting these ideas, we suggest the following interpretation of our results. In solution, a polyelectrolyte molecule exists as a swollen statistical coil, the size of which depends on the polyelectrolyte charge and ionic strength. Upon adsorption it partially loses its solution conformation as schematically shown in Figure 8. Due to the strong electrical field near the surface and the nonelectrostatic interactions, the bulk conformation of the part of the molecule which first comes into contact with the surface collapses. Further conformational rearrangements of the molecule and its spreading over the surface will be kinetically prevented since the molecule has already formed multiple anchoring with the surface which makes its interfacial conformation “frozen”. Moreover, the spreading is possibly also hampered by adsorption of neighboring molecules. As a consequence, a substantial portion of the molecule will not be involved in the immediate interaction with the surface. By contrast, in the theory the equilibrium condition implies a further spreading and a smaller extension of the molecules into solution. In reality, perhaps, such a situation can be reached only if unlimited time is given for reconformation.

As a result, the equilibrium theory is expected to underestimate the surface charge overcompensation and, in general, the adsorbed amount. At the same time, the composition of the thin layer next to the surface can be well described by the theory in the case of an adequate treatment of electrostatic and nonelectrostatic interactions of the polyelectrolyte with the substrate.

This picture of an adsorbed polyelectrolyte kinetically trapped is supported by a number of the trends observed in the experiments. (i) The increase of the adsorbed amount with increasing electrolyte concentration is naturally explained by the shrinking of the polyelectrolyte molecules so that more of them can be accommodated on the surface (see Figure 8a). (ii) Since the surface charge compensation occurs in a thin layer adjacent to the surface, the degree of the molecule collapse should depend on the surface charge as depicted in Figure 8b. This explains why the adsorbed amount reaches a plateau while the surface charge is still growing, as in case of the silica surface. The plateau is reached when the adsorbed layer is filled with polyelectrolyte, but the neutralization of the growing surface charge still can be achieved via progressive collapse of the polyion onto the surface. (iii) The degree of the collapse will also depend on the expansion of the molecule in solution. At a high polyelectrolyte charge and low ionic strength, spreading of the molecule at the surface can be expected to be at its highest, and at these conditions one should expect a better agreement between experiment and the theory as observed for system 2 at $c_s = 0.001$ M.

To conclude, it is widely accepted that equilibrium is seldom, if ever, achieved for polyelectrolyte adsorption at oppositely charged surfaces and we believe that a large fraction of remaining discrepancies between experimental and theoretical results is due to the nonequilibrium behavior of real systems. Further assessment of the kinetical barriers for achieving equilibrium adsorption of polyelectrolytes at charged surfaces from solution could be obtained by slow variation and cycling of pH and electrolyte concentration or by slow increase of the polyelectrolyte concentration from very dilute solutions.

Acknowledgment. We thank Barry Ninham for valuable discussions. This work has been supported by grants from the Swedish National Research Council (NFR) and the Swedish Research Council for Engineering Science (TFR).

References and Notes

(1) Fleer, G. J.; Cohen Stuart, M. A.; Scheutjens, J. M. H. M.; Cosgrove, T.; Vincent, B. *Polymers at Interfaces*; Chapman & Hall: London, 1993.
(2) Hesselink, F. T. *J. Colloid Interface Sci.* **1977**, *60*, 448.
(3) Åkesson, T.; Woodward, C.; Jönsson, B. *J. Chem. Phys.* **1989**, *91*, 2461.
(4) Israëls, R.; Scheutjens, J. M. H. M.; Fleer, G. J. *Macromolecules* **1993**, *26*, 5405.
(5) Borisov, O. V.; Zhulina, E. B.; Birshtein, T. M. *J. Phys. II* **1994**, *4*, 913.
(6) Muthukumar, M. *J. Chem. Phys.* **1987**, *86*, 7230.
(7) Evers, O. A.; Fleer, G. J.; Scheutjens, J. M. H. M.; Lyklema, J. *J. Colloid Interface Sci.* **1986**, *111*, 446.
(8) Varoqui, R.; Johner, A.; Elaissari, A. *J. Chem. Phys.* **1991**, *94*, 6873.
(9) Borukhov, I.; Andelman, D.; Orland, H. *Europhys. Lett.* **1995**, *32*, 499.
(10) Linse, P. *Macromolecules* **1996**, *29*, 326.
(11) Böhmer, M. R.; Evers, O. A.; Scheutjens, J. M. H. M. *Macromolecules* **1990**, *23*, 2288.
(12) van de Steeg, H. G. M.; Cohen Stuart, M. A.; de Keizer, A.; Bijsterbosch, B. *Langmuir* **1992**, *8*, 2538.
(13) Shubin, V.; Linse, P. *J. Phys. Chem.* **1995**, *99*, 1285.
(14) Beltrán, S.; Hooper, H. H.; Blanch, H. W.; Prausnitz, J. M. *Macromolecules* **1991**, *24*, 3178.
(15) Wallin, T.; Linse, P. *Langmuir* **1996**, *12*, 305.
(16) Israëls, R. PhD Thesis, Wageningen University, 1994.
(17) Scheutjens, J. M. H. M.; Fleer, G. J. *J. Phys. Chem.* **1979**, *83*, 1619.
(18) Scheutjens, J. M. H. M.; Fleer, G. J. *J. Phys. Chem.* **1980**, *84*, 178.
(19) Blaakmeer, J.; Böhmer, M. R.; Cohen Stuart, M. A.; Fleer, G. J. *Macromolecules* **1990**, *23*, 2301.
(20) Papenhuijzen, J.; Fleer, G. J.; Bijsterbosch, B. H. *J. Colloid Interface Sci.* **1985**, *104*, 553.
(21) van de Steeg, H. G. M.; de Keizer, A.; Cohen Stuart, M. A.; Bijsterbosch, B. H. *Colloids Surf. A: Physicochem. Eng. Aspects* **1993**, *70*, 77.
(22) Ninham, B. W.; Parsegian, A. V. *J. Theor. Biol.* **1971**, *31*, 405.
(23) Levine, S.; Smith, A. L. *Discuss. Faraday Soc.* **1971**, *52*, 290.
(24) Healy, T. W.; White, L. R. *Adv. Colloid Interface Sci.* **1978**, *9*, 303.
(25) Davis, J. A.; James, R. O.; Leckie, J. O. *J. Colloid Interface Sci.* **1978**, *63*, 480.
(26) Davis, A.; Leckie, J. O. In *Chemical Modelling in Aqueous Systems*; Jenne, E. A., Ed.; American Chemical Society: Washington, DC, 1979; Chapter 15.
(27) James, R. O.; Parks, G. A. In *Chemical Modelling in Aqueous systems*, Jenne, E. A., Ed.; American Chemical Society: Washington, DC, 1979; Chapter 15.
(28) Koopal, L. K.; van Riemsdijk, W. H.; Roffey, M. G. *J. Colloid Interface Sci.* **1987**, *118*, 117.
(29) Bonekamp, B. C.; Lyklema, J. *J. Colloid Interface Sci.* **1986**, *113*, 67.
(30) Sidorova, M. P.; Golub, T. P.; Musabekov, K. *Adv. Colloid Interf. Sci.* **1993**, *43*, 1.
(31) Hoogeveen, N. G.; Stuart, M. A. C.; Fleer, G. J. *J Colloid Interface Sci* **1996**, *182*, 133.
(32) Shubin, V. Submitted for publication in *J. Colloid Interface Sci.*
(33) Shubin, V.; Samoshina, Y.; Menshikova, A.; Evseeva, T. *Colloid Polym. Sci.*, in press.
(34) Dupont, L.; Foissy, A. *Colloid Surf. A* **1996**, *110*, 235.
(35) James, R. O.; Parks, G. A. In *Surface and Colloid Science*; Matijević, E., Ed; Plenum: New York, 1982; Vol. 12, p 119.
(36) Micka, U.; Kremer, K. *Phys. Rev. E* **1996**, *54*, 2653.
(37) Shubin, V.; Kékicheff, P. *J. Colloid Interface Sci.* **1993**, *155*, 108.
(38) Cabani, S.; Gianni, P.; Mollica, V.; Lepori, L. *J. Solution Chem.* **1981**, *10*, 563.
(39) Tadros, T. F.; Lyklema, J. *J. Electroanal. Chem.* **1968**, *17*, 267.
(40) Tanaka, H.; Ödberg, L.; Wågberg, L.; Lindström, T. *J. Colloid Interface Sci.* **1990**, *134*, 219.
(41) Eriksson, L.; Alm, B.; Stenius, P. *Colloids Surf., A* **1993**, *70*, 47.
(42) Vandeven, T. G. M. *Adv. Colloid Interface Sci.* **1994**, *48*, 121.
(43) Hoogeveen, N. G.; Stuart, M. A. C.; Fleer, G. J. *J. Colloid Interface Sci.* **1996**, *182*, 146.
(44) Scales, P. J.; Grieser, F.; Healy, T. W.; White, L. R.; Chan, D. Y. C. *Langmuir* **1992**, *8*, 965.

MA970334H